PORT SAID ENGINEERING RESEARCH JOURNAL

Faculty of Engineering - Port Said University
Volume 29 No. 3 pp: 1:17

Higher Order Beam-Column Element for Inelastic Analysis of Steel Frames Considering Plasticity Spread

Abbad-Elrahman Farag [1], Tarek Sharaf[2], Mohamed Elghandour[3], Ashraf El-Sabbagh[4]*

[1] *Civil Engineering Department, Faculty of Engineering, Port Said University, Port Said, Egypt, email: abbad.farg@gmail.com*

[2] *Civil Engineering Department, Faculty of Engineering, Port Said University, Port Said, Egypt, email: tarek.sharf @eng.psu.edu.eg.com*

[3] *Civil Engineering Department, Faculty of Engineering, Port Said x University, Port Said, Egypt, email: drelghandor@gmail.com*

4 *Civil Engineering Department, Faculty of Engineering,* Port Said *University,* Port Said, Egypt, *email: ashref.ismail @eng.psu.edu.eg.com*

**Corresponding author, DOI: 10.21608/pserj.2025.340870.1382*

Received 1-12-2024,
Revised 20-3-2025,
Accepted 14-4- 2025

ABSTRACT

This work presents a beam-column model for advanced analysis of steel frames. Tracing the effects of both geometric and material nonlinearities requires significant computational effort to maintain the accuracy of the analysis. The proposed element helps resolve the conflict between analysis accuracy and the number of required calculations by representing the physical steel member with a single element. Many existing studies present one-element-per-member models, but they assume lumped plasticity at the element's nodes only, using plastic hinge analysis. In contrast, the present work is based on distributed plasticity analysis using one element per member, which provides a more realistic modeling of steel frames with fewer calculations. A fifth-order shape function is adopted to capture and model second-order effects. Numerical verifications are presented to demonstrate the accuracy of the proposed element by solving numerous benchmark frames and other examples under various loading conditions.

Keywords: Distributed plasticity, Space Steel Frames, Advanced analysis, Higher Order Element, Geometric Nonlinearity

1 INTRODUCTION

With the ongoing progress of employing different software facilities in the analysis and design of steel frames, the concept of advanced analysis gained more importance and attracted the researchers for years. Advanced analysis enabled structural engineers to perform accurate structural analysis that considers many effects were neglected before. First order elastic analysis neglects many effects that affect the behaviors of the steel frames such as geometric nonlinearity, plasticity spread, residual stresses, initial out of straightness and joints semi rigidity. The neglected effects mentioned raise the degree of uncertainty about the structural manner, and consequently the required safety factor rises which may produce uneconomic design.

The concept of advanced analysis is based on considering the effects that were neglected before by incorporating them into the analysis process, which reduces uncertainties about structural behavior and can help achieve more economic and safe designs. Many design specifications allow the use of advanced analysis to design steel frames [1], which provides more realistic modeling for more reliable, safe, and economic designs.

The research on developing appropriate models for structural analysis began earlier, with many researchers attempting to provide an accurate representation of the frame behavior under different effects [2-4]. One of the main effects is the spread of plasticity in steel-framed structures. Unlike elastic analysis, which considers the yield stress as a failure point, inelastic analysis explores the behavior of the structure after the yielding of its elements. To capture the effects of plasticity during analysis, two main concepts were developed: plastic

hinge and plastic zone. Plastic hinge analysis assumes that plasticity occurs only at member nodes, while the rest of the member remains in the elastic stage [5, 6]. Plastic zone analysis assumes plasticity is spread along the entire length of the member, which is more realistic and accurate but comes with additional computational costs [7, 8]. To avoid the complexity of plastic zone analysis, many researchers have attempted to provide different methodologies based on the plastic hinge approach.

Unlike the sudden change in ordinary plastic hinges, the method of the refined plastic hinge (RPH) assumes the yielding at the section to be gradual, meaning the stiffness of the member changes gradually during the analysis. Earlier**,** Liew and Chen [11] investigated the concept of RPH, and due to its advantages, many researchers have adopted it for their work. Iu and Bradford [9] employed RPH to trace material nonlinearity with their fourth-order element. Zhou et al. [12] assumed a third hinge to be placed along the span to capture plasticity at different positions. Similarly**,** Dang et al. [10] tried to use the same concept but included joint semi-rigidity in the analysis. Zhou et al**.** [13] presented a refined plastic hinge model that takes the effects of local buckling and strain hardening into consideration. The models based on RPH present good accuracy; however, they still have a major weakness in considering concentrated plasticity.

Plastic zone analysis, which considers distributed plasticity, can be performed using finite element analysis, representing the frame member using a fine mesh of shell or solid elements [1]. Shell or solid elements meshes are accurate and realistic for modelling steel frames, but it requires many calculations and complexity in modelling not appropriate for practical purposes. Therefore, they are usually used in scientific research and are not common in practical applications. Another method for plastic zone is by modelling the physical frame member by a number of beam-column elements, then the cross-section of each element is divided into many fibers, this process of division helps to capture the spread of plasticity along the span. Viana *et al*. [2] employed plastic zone analysis for their dynamic analysis of steel frames. Thai *et al*. [3] employed the distributed plasticity concept to analyze steel frames with semi rigid connections.

The distributed plasticity analysis provides superior accuracy, especially when considering residual stresses [17, 18], this is why research studies tried to find solutions to reduce its required number of calculations which is the main disadvantage. Researchers such as Du *et al.* [6], [7], employed a flexibility-based approach as a different way of analysis that can trace plasticity spread. Also, flexibility-based work was employed by many researchers for tapered element analysis [40, 41]. However, flexibility-based analysis requires integration for the cross-section and along the member which costs more calculations. To save calculations, Zubydan [8] presented new formulas to obtain the section tangent stiffness of H-shaped sections directly without dividing the cross-section into many fiber elements. Elsabbagh *et al*. [9] developed the tangent stiffness formulas for I-shaped sections.

To capture second order effects due to geometric nonlinearity many methodologies have been found. First of all, when representing the member with finite element mesh of shells or solids, the second order effect is traced easily. But when using beam-column element, the accuracy of second-order analysis depends on the formulation of the beam column element. Stability functions found by Oran [10] provided the exact solution of the element considering the interaction between axial force and bending moment, however, it may cause divergence during analysis due to the different expressions for tension and compression cases. Many researchers used stability function in their advanced analysis such as Thai and Kim [11]. Although there was a great accuracy in representing axial flexural interaction by stability functions, researchers tried to find a model based on polynomial shape function to avoid solution divergence. Third order shape function produced a beam-column, well-known as cubic element, that overcame the divergence issue, but the member should be divided into more than one element to maintain the accuracy [12]. To avoid dividing the member, higher order elements were found. Fifth displacement function by Chan and Zhou [13] produced a beam column element that accurately captured second order effects, known as (PEP) element. Also, Iu and Bradford [14] developed their own element based on a fourth order shape function and merged it with plastic hinge approach [15].

The main dilemma was the direct incremental relationship between the accuracy and the required calculations. Zubydan *etal*. [16] produced their equivalent accumulated element which attempts to merge fourth order element with plasticity spread analysis without dividing the member. Their work has the limitations of fourth order element in geometric nonlinearity. For practical beam-column element analysis, most researchers incorporate stability functions or higher order elements with plastic hinge approach to represent the member using one element [17], but it neglected yielding along the span.

The present work aims to provide a beam-column model using fifth order shape function and integrating it with the plasticity spread approach using one element per member. This approach helps to maintain the accuracy of tracing geometric and material nonlinearities. The used one element concept helps in saving size of matrices and calculation efforts. Unlike the other research studies that use cubic or fourth-shape function, the present work uses the fifth-order shape function which maintain the accuracy even with high slenderness ratios of frames. Also, for second order stiffens coefficients, the present work tries to enhance the ability of modelling high slenderness member by considering appropriate

equivalent rigidity. The element's ability to trace moderately large deformations is going to be strengthened. The presented numerical examples demonstrate the superiority of the present work comparing to conventional cubic elements and plastic hinge approaches.

2 ASSUMPTIONS AND SHAPE FUNCTIONS

This section provides explanation of the adopted assumptions, and compares the capabilities of fourth and fifth order shape functions for second-order elastic analysis. As the present work is dedicated to higher order functions, the cubic function will not be discussed.

2.1 Assumptions

During derivation of the element is based on main assumptions.

- Sections always are plane even after deformation
- Local buckling and lateral torsional buckling are not allowed.
- Shear deformation and warping effects are neglected, and members have bisymmetrical cross sections.
- Loads are assumed to be nodal only.
- Strain hardening of steel material is neglected.
- Large rotations and displacements with small strains are considered

2.2 Fourth Order Shape Function

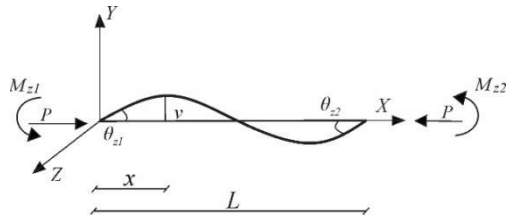

(a)

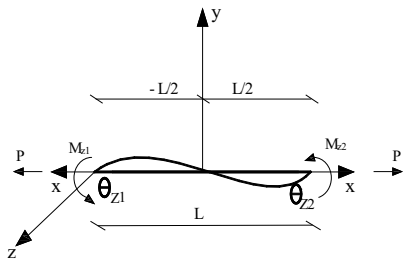

(b)

Figure 1: Member in Equilibrium; a) X=0 to L, b) X=-L/2 to L/2

The frame element shown in Figure 1 assumes the same presented assumptions, and the fourth order shape function deduced by [14] used five boundary conditions based on the equilibrium in Figure 1.a where x ranges from 0 to L. The five boundary conditions are the values of displacements and bending moment at both ends, and also the value of bending moment at the mid span of the element to derive the fourth order function in Eq.1

$$v = \left[\xi - \frac{4(24+q)}{48+q}\xi^2 + \frac{48+5q}{48+q}\xi^3 - \frac{2q}{48+q}\xi^4\right]L\theta_{z1} + \left[-\frac{48-q}{48+q}\xi^2 + \frac{3(16-q)}{48+q}\xi^3 + \frac{2q}{48+q}\xi^4\right]L\theta_{z2} \quad (1)$$

Where, $q = PL^2/EI_z$ and $\xi = x/L$.

The displacement function presented in Eq.1 was used in [14] for elastic second order analysis, in [15] for concentrated plasticity analysis, and in [16] for distributed plasticity analysis. The deduced elastic stiffness coefficients are the same for both tension and compression cases, however, its accuracy decreases comparing to exact solutions of stability functions when the axial load factor q reaches high levels.

2.3 Fifth Order Shape Function

The fifth order shape function, which is adopted in the current research, was deduced in [13] depending on the frame under equilibrium, shown in Figure 1.b, considering the axis to start from mid span and x ranges from *-L/2* to *L/2*. The difference is they considered six boundary conditions, that are the values of displacements and moment at element nodes, and the values of shear force and bending moment at midspan point. The additional condition of shear force value enabled the shape function to get higher order than the fourth.

For the present work a fifth order shape function is going to be deduced to consider the element in equilibrium as shown in Figure 1.a, where x ranges from 0 to L, to make the function applicable in the coming derivations.

After applying the boundary conditions on the equilibrium of the element in Figure 1.a, a fifth order shape function is driven as shown in Eq.2.

$$v = L\theta_{z1}\left[\xi - \frac{0.5(5q+48)\xi^2}{q+48} + \frac{(4q)\xi^3}{q+48} - \frac{(2q)\xi^4}{q+48} - \frac{0.5(7q+240)\xi^2}{q+80} + \frac{(80+9q)\xi^3}{q+80} - \frac{(10q)\xi^4}{q+80} + \frac{(4q)\xi^5}{q+80}\right] \quad (2)$$

$$+ L\theta_{z2}\left[\frac{0.5(5q+48)\xi^2}{q+48} - \frac{(4q)-\xi^3}{q+48} + \frac{(2q)\xi^4}{q+48} - \frac{0.5(7q+240)\xi^2}{q+80} + \frac{(80+9q)\xi^3}{q+80} - \frac{(10q)\xi^4}{q+80} + \frac{(4q)\xi^5}{q+80}\right]$$

Where, $q = PL^2/EI_z$ and $\xi = x/L$.

The elastic second order stiffness coefficients from fifth order function resulted a stable model in the analysis that does not cause divergence issues while maintaining acceptable accuracy. Many researchers tried to use this model during plastic analysis by combining it with plastic hinge approach. A key contribution of the present research is to merge the fifth order element with plastic zone approach to achieve a high accuracy in tracing both geometric and material nonlinearities.

3 NUMERICAL DERIVATION

This section presents the numerical derivation of the beam column element by deducing secant relations and ending to tangent stiffens matrix. An explanation of the main methodology of tracing plasticity spread is presented in Section 3.1. The secant relations are deduced in two steps. Firstly, the first order relations are presented in Section 3.2, after that the second order effect is included in the derivation by two different methods each of them provides a different numerical model can be used. So, the numerical verifications contain results of two models.

3.1 The Equivalent Accumulated Element

During inelastic analysis, the internal forces acting on cross sections escalate with the increasing of loading process. These internal forces can make some fibers of the steel element to yield. For any cross section with yielded parts, the value of sectional rigidity decreases due to plasticity spread, consequently the whole stiffness of the member degrades. The main concept of the equivalent accumulated element is to represent the frame element by one element and this element has a number of internal segments. Each internal segment is allowable to have different section rigidity, and this rigidity can be calculated by monitoring its start and end sections. The internal forces at the monitored cross sections are calculated, throughout the analysis process. The rigidity of the cross sections is evaluated based on the internal forces.

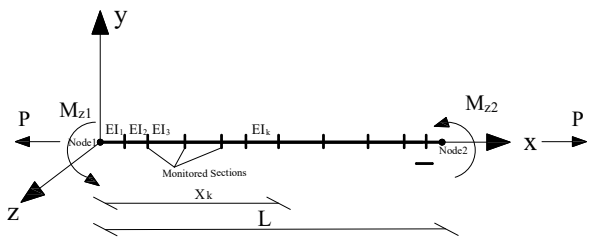

Figure 2: Member under equilibrium with different values of *EI*

Section 4 provides additional illustrations on the evaluation of the cross sections. The degraded internal segments due to plasticity cause the element to have segments with different values of EI, as shown in Figure2. The aim of this section is to provide stiffness first and second order coefficients for that element.

3.2 First Order Relations

Firstly, the first order stiffness for the member with variable segments has been provided in [16] based on Castigliano's second theorem. When considering P=0, the bending moment equation $M_z = M_{z1}(1-\xi) - M_{z2}\,\xi$ is used to get strain energy. Based on the strain energy function in Eq.3, the end rotations can be found by differentiating the energy with respect to the corresponding forces.

$$\mathrm{U} = \int_0^1 \frac{M_z^2}{2EI_z} L d\xi \tag{3}$$

$$\theta_{z1} = \frac{\partial \mathrm{U}}{\partial M_{z1}} = \int_0^1 \frac{M}{EI_z}\frac{\partial M_z}{\partial M_{z1}} L d\xi \tag{4}$$

$$\theta_{z2} = \frac{\partial \mathrm{U}}{\partial M_{z2}} = \int_0^1 \frac{M}{EI_z}\frac{\partial M_z}{\partial M_{z2}} L d\xi \tag{5}$$

When performing the integration in parts and each part has its own EI_z, a rearrangement can be implemented in the expressions to get the secant relations presented from Eq.6 to Eq.13. The coefficients were derived based on the previously mentioned assumptions and they are exact for first-order analysis. These coefficients don't account for the interaction between axial and flexural effects. The first order secant relations for a member bent about z axis are presented in Eq.3 to Eq.10.

$$M_{z1} = C_{mz1}\,\theta_{z1} + C_{mz3}\,\theta_{z2} \tag{6}$$

$$M_{z2} = C_{mz3}\,\theta_{z1} + C_{mz2}\,\theta_{z2} \tag{7}$$

$$C_{mz1} = \frac{-S_{mz1}}{S_{mz3}^2 - S_{mz1}S_{mz2}} \tag{8}$$

$$C_{mz2} = \frac{-S_{mz2}}{S_{mz3}^2 - S_{mz1}S_{mz2}} \tag{9}$$

$$C_{mz3} = \frac{S_{mz3}}{S_{mz3}^2 - S_{mz1}S_{mz2}} \tag{10}$$

$$S_{mz1} = L\sum_{k=1}^{n} \frac{1}{EI_{zk}} \left((\xi_k - \xi_{k-1}) - (\xi_k^2 - \xi_{k-1}^2) + \frac{1}{3}(\xi_k^3 - \xi_{k-1}^3) \right) \quad (11)$$

$$S_{mz2} = L\sum_{k=1}^{n} \frac{1}{EI_{zk}} \left(\frac{1}{3}(\xi_k^3 - \xi_{k-1}^3) \right) \quad (12)$$

$$S_{mz3} = L\sum_{k=1}^{n} \frac{1}{EI_{zk}} \left(-\frac{1}{2}(\xi_k^2 - \xi_{k-1}^2) + \frac{1}{3}(\xi_k^3 - \xi_{k-1}^3) \right) \quad (13)$$

Where $\boldsymbol{\xi_k} = X_k/L$

It's worth mentioning that the expressions don't require the segments to be equal in length. Additionally, the change in segment rigidity can be random, without any restriction, unlike tapered member work. It's noticed that, the presented formulas can model stepped element in elastic linear analysis. Also, all the factors provided can be calculated simply by accumulating process for all member segments.

3.3 Secant Relations Including Second Order Effects

At this stage of the derivation the modified fifth order displacement function, in Eq.2, is going to be employed along with the secant stiffness coefficients. The first model will be based on the second theorem of Castigliano in Section 3.3.1, and the second model uses a direct replacement technique to deduce the coefficients. Both models are tested through numerical examples to assure their accuracy.

3.3.1 First Model of Fifth Order Shape Function

The present model considers the equilibrium of frame element shown in Figure 2, considering the value of $P \neq 0$. The expression of shear force at node 1 can be represented as a function of $M_{z1}, M_{z2}, and\ L$. So, the expression for the bending moment along the member can be written as shown in Eq. 14.

$$\mathrm{M}_z = M_{z1}(1-\xi) - M_{z2}\,\xi - P\,v \quad (14)$$

Where $\boldsymbol{\xi} = X/L$, and $\boldsymbol{v}$ is the shape function in Eq. 2.

To employ Castigliano's second theorem, the strain energy expressed in Eq.3 is employed but this time with the equation of bending moment in Eq.14. So, we can get expressions for end rotations by differentiating strain energy with respect to $M_{z1}\ and\ M_{z2}$. After substituting by the equation of moment and its differentiations about $M_{z1}\ and\ M_{z2}$, the expressions for end rotations are found, as presented in Eq.15 and Eq.16. The differentiation of equation of moment neglects the dedifferentiation of the term Pv with respect to $M_{z1}\ and\ M_{z2}$.

$$\theta_{z1} = \frac{\partial \mathrm{U}}{\partial M_{z1}} = \int_0^1 \frac{(M_{z1}(1-\xi) - M_{z2}\,\xi - P\,v)\,(1-\xi)}{EI_{zk}}\,Ld\xi \quad (15)$$

$$\theta_{z2} = \frac{\partial \mathrm{U}}{\partial M_{z2}} = \int_0^1 \frac{(M_{z1}(1-\xi) - M_{z2}\,\xi - P\,v)\,(-\xi)}{EI_{zk}}\,Ld\xi \quad (16)$$

To perform the integration, it's essential to take different values of EI_z into consideration. So, integration in parts is going to be performed and that makes the expressions as follows.

$$\theta_{z1} = \sum_{k=1}^{n} \int_{\xi_{k-1}}^{\xi_k} \frac{(M_{z1}(1-\xi) - M_{z2}\,\xi - P\,v)\,(1-\xi)}{EI_{zk}}\,Ld\xi \quad (17)$$

$$\theta_{z2} = \sum_{k=1}^{n} \int_{\xi_{k-1}}^{\xi_k} \frac{(M_{z1}(1-\xi) - M_{z2}\,\xi - P\,v)\,(-\xi)}{EI_{zk}}\,Ld\xi \quad (18)$$

The expressions in Eq.17 and Eq.18 can be specified and separated according to three parameters, $M_{z1}, M_{z2}, and\ Pv$. The term related to Pv represents the effects of geometric nonlinearity, while the terms related to $M_{z1}\ and\ M_{z2}$ are related to first order coefficients. The terms containing Pv will be integrated directly from 0 to 1 considering one approximate value of rigidity EI_{eq},for simplification, which will be discussed later in section 4 and different methods will be presented for it.

$$\theta_{z1} = M_{z1}S_{mz1} + S_{gz1}\,\theta_{z1} + M_{z2}S_{mz3} + S_{gz3}\,\theta_{z2} \quad (19)$$

$$\theta_{z2} = M_{z1}S_{mz1} + S_{gz2}\,\theta_{z2} + M_{z2}S_{mz2} + S_{gz4}\,\theta_{z1} \quad (20)$$

$$\theta_{z2} = M_{z1}S_{mz1} + S_{gz2}\,\theta_{z2} + M_{z2}S_{mz2} + S_{gz4}\,\theta_{z1} \quad (21)$$

Where the factors $\boldsymbol{S_{mz1}}\ to\ \boldsymbol{S_{mz3}}$ will be the same as Eq.11 to Eq.13. The parts $S_{gz1}\ to\ S_{gz4}$ are as following.

$$S_{gz1} = \frac{PL^2}{EI_{eqz}} \int_0^1 \left(-\left(\xi - \frac{0.5(5q+48)\xi^2}{q+48} + \frac{(4q)\xi^3}{q+48} - \frac{(2q)\xi^4}{q+48} - \frac{0.5(7q+240)\xi^2}{q+80} + \frac{(80+9q)\xi^3}{q+80} - \frac{(10q)\xi^4}{q+80} + \frac{(4q)\xi^5}{q+80} \right) (1-\xi) \right) d\xi \quad (22)$$

$$S_{gz2} = \frac{PL^2}{EI_{eqz}} \int_0^1 \left(-\left(\frac{0.5(5q+48)\xi^2}{q+48} - \frac{(4q)-\xi^3}{q+48} + \frac{(2q)\xi^4}{q+48} - \frac{0.5(7q+240)\xi^2}{q+80} + \frac{(80+9q)\xi^3}{q+80} - \frac{(10q)\xi^4}{q+80} + \frac{(4q)\xi^5}{q+80} \right) (-\xi) \right) d\xi \quad (23)$$

$$S_{gz3} = \frac{PL^2}{EI_{eqz}} \int_0^1 \left(-\left(\xi - \frac{0.5(5q+48)\xi^2}{q+48} + \frac{(4q)\xi^3}{q+48} - \frac{(2q)\xi^4}{q+48} - \frac{0.5(7q+240)\xi^2}{q+80} + \frac{(80+9q)\xi^3}{q+80} - \frac{(10q)\xi^4}{q+80} + \frac{(4q)\xi^5}{q+80} \right) (-\xi) \right) d\xi \quad (24)$$

$$S_{gz4} = \frac{PL^2}{EI_{eqz}} \int_0^1 \left(-\left(\frac{0.5(5q+48)\xi^2}{q+48} - \frac{(4q)-\xi^3}{q+48} + \frac{(2q)\xi^4}{q+48} - \frac{0.5(7q+240)\xi^2}{q+80} + \frac{(80+9q)\xi^3}{q+80} - \frac{(10q)\xi^4}{q+80} + \frac{(4q)\xi^5}{q+80} \right) (1-\xi) \right) d\xi \quad (25)$$

At this level, we can perform the integration as previously mentioned and solve the equations 19 and 20 with each other's to get final secant moment relations as following.

$$M_{z1} = \left(C_{mz1} + C_{gz1}\right) \theta_{z1} + \left(C_{mz3} + C_{gz2}\right) \theta_{z2} \quad (26)$$

$$M_{z2} = \left(C_{mz3} + C_{gz2}\right) \theta_{z1} + \left(C_{mz2} + C_{gz1}\right) \theta_{z2} \quad (27)$$

Where $C_{mz1}, C_{mz2}, and\ C_{mz3}$ are the (Maml as presented in Eq.8 to Eq.13, $\theta_{z1} = \int_0^1 \frac{M_{z1}(1-\xi) - M_{z2}\,\xi}{EI_z}$ (1 and the factors $C_{gz1}\ and\ C_{gz2}$ are expressed in Eq.28 and Eq.29.

$$C_{gz1} = \frac{EI_{eqz}}{L}\left(\frac{\frac{4q^3}{105} + \frac{1088q^2}{105} + 512q}{q^2 + 128q + 3840} \right) \quad (28)$$

$$C_{gz2} = \frac{EI_{eqz}}{L}\left(\frac{\frac{q^3}{210} - \frac{32q^2}{105} - 128q}{q^2 + 128q + 3840} \right) \quad (29)$$

For a three-dimensional frame, the previous work can be deduced for the bending about y axis and get secant stiffness corresponding to $M_{y1}\ and\ M_{y2}$. As explained in Section 4, the used corotational procedure of analysis, guarantees that the displacements in the three-dimensional work are transformed accurately. $\theta_{z2} = \int_0^1 \frac{M_{z1}(1-\xi) - M_{z2}\,\xi}{EI_z}$ (-

3.3.2 Second Model of Fifth Order Shape Function

A different methodology can be used to employ higher-order function with plasticity spread models. The steps of this method depend on finding the elastic secant stiffness of the element considering both first- and second-order effects. As the member is still elastic, the first-order coefficients separately are known as $4EI_z/L$ and $2EI_z/L$. These elastic stiffness coefficients for the fifth order function have been found previously in [13] as presented in Eq. 30 to Eq. 33.

$$M_{z1} = (C_{z1}\theta_{z1} + C_{z3}\theta_{z2}) \quad (30)$$

$$M_{z2} = (C_{z3}\,\theta_{z1} + C_{z2}\theta_{z2}) \quad (31)$$

$$C_{z1} = C_{z2} = \frac{EI_z\left(19200 + 800q + \frac{61}{7}q^2 + \frac{23}{1260}q^3\right)}{L(q+80)^2} + \frac{EI_z\left(2304 + 288q + \frac{29}{5}q^2 + \frac{11}{420}q^3\right)}{L(q+48)^2} \quad (32)$$

$$C_{z3} = \frac{EI_z\left(19200 + 800q + \frac{61}{7}q^2 + \frac{23}{1260}q^3\right)}{L(q+80)^2} - \frac{EI_z\left(2304 + 288q + \frac{29}{5}q^2 + \frac{11}{420}q^3\right)}{L(q+48)^2} \quad (33)$$

In the present work, the first-order stiffness coefficients found in equations 8 to 13 can include plasticity spread effects. Therefore, we will subtract elastic first-order coefficients $4EI_z/L$, $4EI_z/L$, and $2EI_z/L$ from the expressions C_{z1}, C_{z2}, and C_{z3} in Eq.32 and Eq.33, then replace them with the degraded first order coefficients $C_{mz1}, C_{mz2}, and\ C_{mz3}$ which include the

effects of plasticity spread inherent in the variation of sections rigidity due to yielding. The final secant coefficients C_{z1}, C_{z2}, and C_{z3} after modifications for second-order inelastic analysis can be expressed as follows.

$$C_{z1} = \mathrm{C_{mz1}} + \frac{EI_{eqz}}{L}\left(\frac{\left(\frac{23q^3}{1260}+\frac{40q^2}{7}+320q\right)}{(q+80)^2} + \frac{\left(\frac{11q^3}{420}+\frac{24q^2}{5}+192q\right)}{(q+48)^2}\right) \quad (34)$$

$$C_{z2} = \mathrm{C_{mz2}} + \frac{EI_{eqz}}{L}\left(\frac{\left(\frac{23q^3}{1260}+\frac{40q^2}{7}+320q\right)}{(q+80)^2} + \frac{\left(\frac{11q^3}{420}+\frac{24q^2}{5}+192q\right)}{(q+48)^2}\right) \quad (35)$$

$$C_{z3} = \mathrm{C_{mz3}} + \frac{EI_{eqz}}{L}\left(\frac{\left(\frac{23q^3}{1260}+\frac{40q^2}{7}+320q\right)}{(q+80)^2} - \frac{\left(\frac{11q^3}{420}+\frac{24q^2}{5}+192q\right)}{(q+48)^2}\right) \quad (36)$$

3.4 Tangent Stiffness Matrices

In the present work, an evaluation process to the capacity of the cross section is performed each loading increment. This evaluation process finds a new degraded rigidity for the cross section if any plasticity spread is found at the cross section. Section 4 illustrates the analysis procedure, including how the rigidity is evaluated. When the monitored sections have different values of EI, each internal segment will have its own value of EI. This means the plasticity spread is inherent already in the stiffness coefficients, and the tangent stiffness matrix can be found directly as if the member was elastic but with variable stiffness.

Two main beam-column models have been presented in this paper. The first is based on the expressions deduced

in Section 3.3.1, and the second model is based on expressions in Section 3.3.2. Tangent stiffness matrix can be found in Eq.30, but it must be notified that the difference between model 1 and model 2 will be related to the used values of expressions of $C_{\mathrm{zii}}, C_{\mathrm{zij}}, and\ C_{\mathrm{zij}}$. The bowing functions related to fifth order shape function are employed to calculate factors like $G_{1\alpha}$, $G_{2\alpha}$ and H_α which are the same for both modes.

$$G_{1\alpha} = 2b_1(\theta_{1\alpha}+\theta_{2\alpha}) + 2b_2(\theta_{1\alpha}-\theta_{2\alpha}) \quad (38)$$

$$G_{2\alpha} = 2b_1(\theta_{1\alpha}+\theta_{2\alpha}) - 2b_2(\theta_{1\alpha}-\theta_{2\alpha}) \quad (39)$$

$$H_\alpha = \frac{I_\alpha}{AL^2} - \sum_{N}^{N=z.y}\frac{I_N}{I_\alpha}\left(b_1'\ (\theta_{1\alpha}+\theta_{2\alpha})^2 + b_2'\ (\theta_{1\alpha}-\theta_{2\alpha})^2\right) \quad (40)$$

$$b_1 = \frac{\left(\frac{23q^3}{2520}+\frac{46q^2}{21}+\frac{2080}{7}q+12800\right)}{(q+80)^3} \quad (41)$$

$$b_2 = \frac{\left(\frac{11q^3}{840}+\frac{66q^2}{35}+\frac{672}{5}q+4608\right)}{(q+48)^3} \quad (42)$$

The symbol α refers to axis z or y. The equation for axial force can be expressed as following.

$$K_T^4 = \begin{pmatrix} c_{zii}+\frac{EI_{eq_z}}{L}\frac{G_{1z}^2}{H_z} & c_{zij}+\frac{EI_{eq_z}}{L}\frac{G_{1z}G_{2z}}{H_z} & \frac{EI_{eq_z}}{L}\frac{G_{1z}G_{1y}}{H_z} & \frac{EI_{eq_z}}{L}\frac{G_{1z}G_{2y}}{H_z} & 0 & \frac{EI_{eq_z}}{L}\frac{G_{1z}}{LH_z} \\ & c_{zjj}+\frac{EI_{eq_z}}{L}\frac{G_{1z}^2}{H_z} & \frac{EI_{eq_z}}{L}\frac{G_{2z}G_{1y}}{H_z} & \frac{EI_{eq_z}}{L}\frac{G_{2z}G_{2y}}{H_z} & 0 & \frac{EI_{eq_z}}{L}\frac{G_{2z}}{LH_z} \\ & & c_{yii}+\frac{EI_{eq_y}}{L}\frac{G_{1y}^2}{H_y} & c_{yij}+\frac{EI_{eq_y}}{L}\frac{G_{1y}G_{2y}}{H_y} & 0 & \frac{EI_{eq_y}}{L}\frac{G_{1y}}{LH_y} \\ & & & c_{yjj}+\frac{EI_{eq_y}}{L}\frac{G_{1y}^2}{H_y} & 0 & \frac{EI_{eq_y}}{L}\frac{G_{2y}}{LH_y} \\ & & symmetrical & & T & 0 \\ & & & & & \frac{EI}{L^3H} \end{pmatrix} \quad (37)$$

$$P = EA\left(\frac{\Delta u}{L} + \sum_{\alpha=y\,z}[b_1(\theta_{\alpha1} + \theta_{\alpha2})^2 + b_2(\theta_{\alpha1} - \theta_{\alpha2})^2]\right) \quad (43)$$

Structure tangent stiffness matrix can be assembled as $K_T = \sum_{elements} L(T^T K_T^4 T)L^T$, where matrices [T] and [L] are to form the [12×12] matrix and to rotate the element from local to global coordinates, respectively. The matrix K_T^4 can be found in Eq. 37, while the matrix T is presented in the appendix. The matrix L for rotating the element can be found in [26].

4 ANALYSIS WORK FLOW

This section illustrates the flow of the analysis, including several issues that need to be discussed to present a complete overview of the workflow of the models.

4.1 Tracing Distributed plasticity

As previously mentioned, this work aims to proceed with the analysis without dividing the member. So, during the analysis, the steel frame member will be represented by only one element with two nodes at start and the end of it. To trace plasticity spread along the span of the member, many sections will be specified along the span, as shown in Figure 3, and these sections will be monitored throughout the analysis process. After each loading variation during the analysis, the straining actions at each monitored section will be calculated, and that will be based on nodal forces, axial force, and element shape function at Eq.2. From the calculated straining actions, a new value for the tangent rigidity EI_t will be found for each monitored section. The evaluation process of the value of EI_t is explained in Section 4.2. Each internal segment of the element is assumed to be located between two monitored sections. The tangent rigidity for each internal segment is found as the average value of EI_t at both monitored sections at the segment limits.

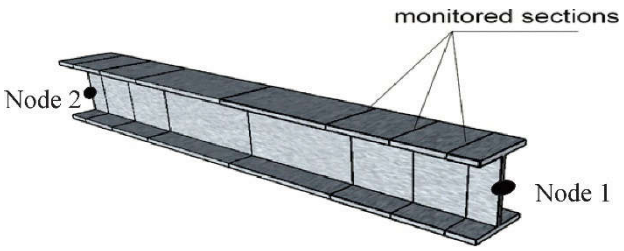

Figure 3: One beam-column element with multi monitored sections

The proposed models in the present work deal with a frame element with multiple internal segments, each of them has different values of EI_t. Therefore, the formed stiffness matrix at Eq.30 contains distributed plasticity effects.

The positioning of monitored sections along the element is vital and needs to get some attention. Anticipation of the plasticity spread should be taken into consideration while allocating the monitored sections. If a zone of the member contains yielded parts and there is no monitored section near to it, the accuracy may be affected. Considering residual stress during the analysis raise the probability of plasticity spread along the span length [4]. For instance, a member with residual stress and axial force is predicted to have a range of plasticity along the span, so a number of monitored section should be found covering the whole member to maintain the accuracy. However, if the member extreme stresses are governed by bending moment values at ends only, the plasticity will be found near the ends only.

4.2 Evaluation of Section Rigidity

To calculate the tangent modulus for a cross-section under certain straining actions, two methodologies can be followed. The first method is discretizing the cross-section into a number of small areas, called fiber model approach. The fiber model approach requires an integration process over the section areas, which consumes more calculation efforts. The second method is to employ direct formulas that can calculate the value of section inelastic rigidity EI_t according to the section dimensions and applied forces. The present work employs direct formulas to evaluate tangent modulus for all monitored sections of the elements. So, the whole procedure of analysis will be based of closed form solutions that do not require internal integration neither across the section area nor along the element length. The formulas found in the research studies [21, 22, 30, 31, 32] are used in the current research as they can cover all cases of H-shaped and I-shaped under different mixes of loadings. Also, these formulas are available for sections considering or neglecting residual stresses.

4.3 Equivalent Stiffness of Members

The derivation in the present research assumed an equivalent value of the rigidity EI_{eq} to be used for the members in calculating second order terms only. This value is allowed to be approximate as the used procedure makes its effect to be limited at the second order terms only, while the first order terms are based on the calculated different values of EI at each monitored section. Although this approximation seems to be limited, the present research suggests two different techniques to consider EI_{eq} to assure the accuracy of model in different circumstances. The numerical examples in Section 5.6 were solved using both of the two methods in Sections 4.31 and 4.32, and no difference in results between them was notified. So, all the presented results in this paper are based on using the

elastic value for second order terms as declared in Section 4.3.1.

4.3.1 Elastic Rigidity Technique

The value of elastic EI is the exact one for the elastic range of loading. When yielding starts to spread, the second order terms start to contain a kind of approximation. However, this approximation will not have a significant effect, as assured by the numerical examples in Section 5. That can be understood by knowing the type of nonlinearity that controls the analysis. When a member has a high slenderness ratio, the geometric nonlinearity governs the analysis and second order terms has a large value. In the previous condition, the buckling occurs while most of the member still elastic and plasticity may be found but concentrated at certain areas. So, the elastic values can be representative for the majority of member. In another case where the member has low slenderness ratio, the plasticity may spread along the member in different, zones and the value of elastic EI loses its accuracy in representing the member. However, the whole values of second order terms are small as plasticity controls the analysis, which means the approximation is trapped in small values with no significant effects on the results. All solved bench marked frames in Section 5 employed the elastic value as EI_{eq}.

4.3.2 Variation of Elastic Load Technique

The elastic load on a segment of the member is the area of bending moment divided by the value of section rigidity. An approximate value of EI_{eq} can be found by equating the value of elastic load of the member with multi-internal segments with the value of elastic load of the member with one approximate EI_{eq}, and that is by applying the equation $\sum(ML_k/EI_k) = (\sum ML_k)/EI_{eq}$ during the analysis extracting a value for EI_{eq} .

4.4 Analysis Scheme

Figure 4 shows the analysis flow chart for the developed software for the analysis. Arch length and minimum residual displacement solution strategies are used to solve the incremental iterative developed procedure. The replicated updating of sections tangent modulus helps in making convergence rabidly in case of inelastic buckling, as it helps to control the unbalance force vector as small as possible.

Throughout the analysis procedure, the incremental equilibrium equation will be as declared in Eq. 44 to start iteration number i at step number j.

$$[K_{i-1}^{j}]\{\Delta u_i^j\} = \{F_{ext\,i}^{j}\} - \{F_{int\,i-1}^{j}\} \quad (44)$$

where, $[K_{i-1}^{j}]$ is the last updated tangent stiffness matrix from iteration number i-1. And $\{\Delta u_i^j\}$ is the generated unbalanced displacement vector after solving the equilibrium condition. The vector $\{\Delta F_{i-1}^{j}\}$ is the last updated internal force vector from previous iteration. The vector $\{F_{ext\,i}^{j}\}$ is the external force vector which can be updated each iteration as the following.

$$\{F_{ext\,i}^{j}\} = \{F_{ext\,i-1}^{j}\} + \Delta\lambda_i^j\,\{\Delta\hat{F}_{ext}\} \quad (45)$$

where, $\{\Delta\hat{F}_{ext}\}$ is the reference load vector. The factor $\Delta\lambda_j^i$ is the load increment factor for the jth iteration in the ith increment, which is calculated according to the adopted nonlinear solution strategy depending on the vectors from previous iteration.

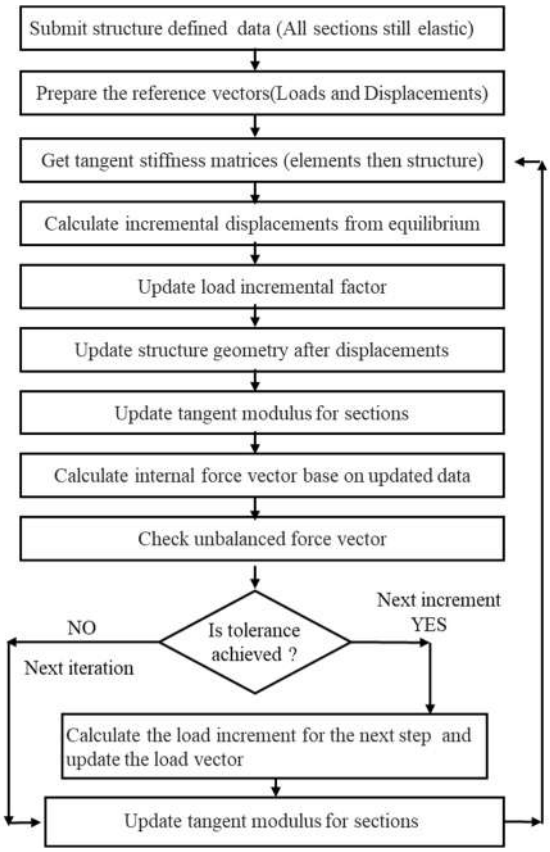

Figure 4: Analysis Flow Chart

5 NUMERICAL EXAMPLES

The numerical examples are in two main categories. The first category examples are the well-known benchmark structures that have solutions, we compare the results of our model with to assess the overall accuracy of the proposed models. Then other examples are provided to assure the availability of the models in cases with wide range of slenderness and plasticity spread.

5.1 One Story Portal Frame

The portal frame in Figure 5 was analyzed by Thai and Kim [21]. They provided accurate solution by meshing the frame to twenty elements per each member using ABAQUS software. The geometry and section dimensions are shown on Figure 5, while the assumed steel material had the Young's modulus E = 19613 MPa and yield stress σy = 98 MPa. The frame is analyzed in the present research using one element for each member. The rectangular cross section has no residual stresses and fiber model is used to evaluate plasticity spread across the area of section. The monitored sections are placed at location 0.05L and 0.1L from both sides of the member as the plasticity is anticipated to be found near ends at this example. The analysis results are presented in Figure 6 and show that the presented models are able to trace geometric and material nonlinearity accurately.

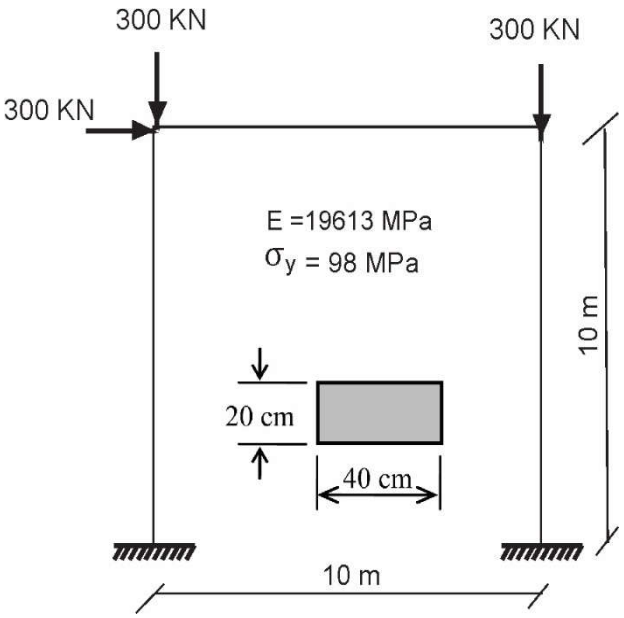

Figure 5: Portal Frame with Rectangular Section

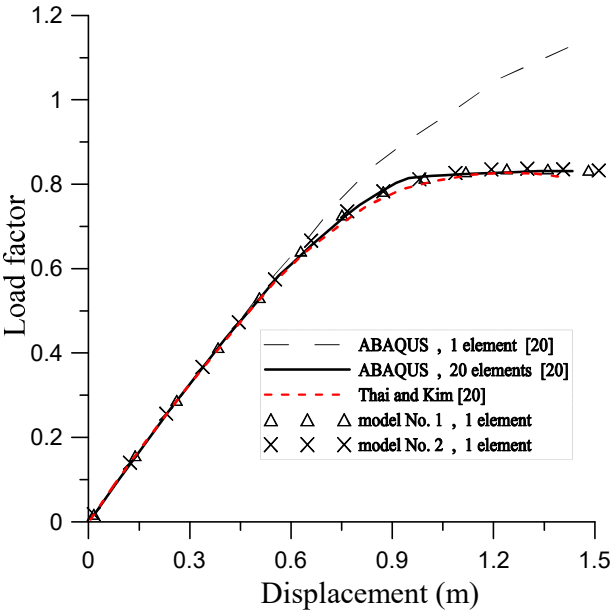

Figure 6: Analysis Results Portal Frame with Rectangular Section

5.2 Multi Story Plan Frame

The plan frame in Figure 7 is a well-known example presented by Vogel [22], as the frame was solved accurately via plastic zone method and accurate solution found. The steel modulus of elasticity is 205 GPa, and the yield stress is 235 MPa. The geometry of frame in Figure 7 is exposed to geometric imperfection, out of plumpness, with an inclination 1/450 for the columns of the six stories.

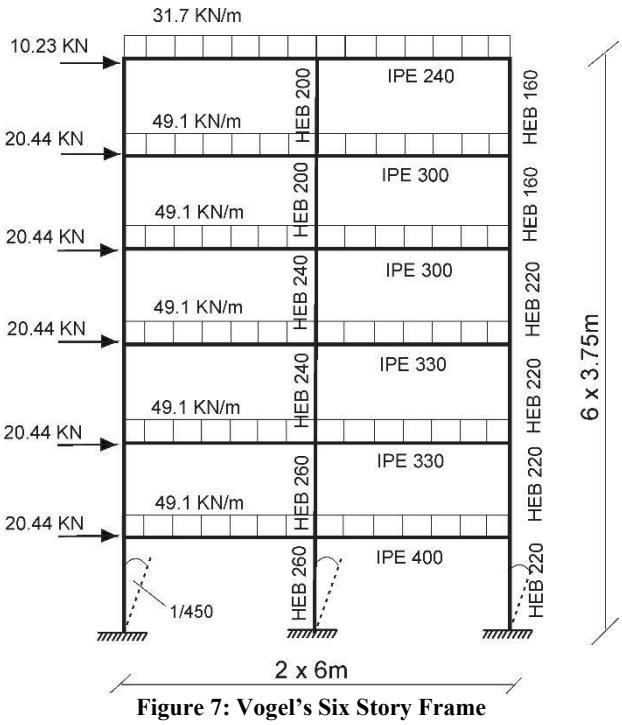

Figure 7: Vogel's Six Story Frame

The main example solved by Vogel had residual stresses as material imperfection. Barasan and Chiorean [5] provided solution for the frame neglecting residual stress during their work on the influence of material nonlinearity. Many other researchers solved the frames with their own models to assure their accuracy, such as the work in [9, 35].

This frame is modeled and solved using the present models to check the reliability of the models. The structure has uniform distributed load on the horizontal element, that's why only beams are modeled as four elements for each beam to be able to add span loads as multi nodal forces. The results shown in Figures 8, 9 reveals the accepted accuracy of the models considering or neglecting residual stresses.

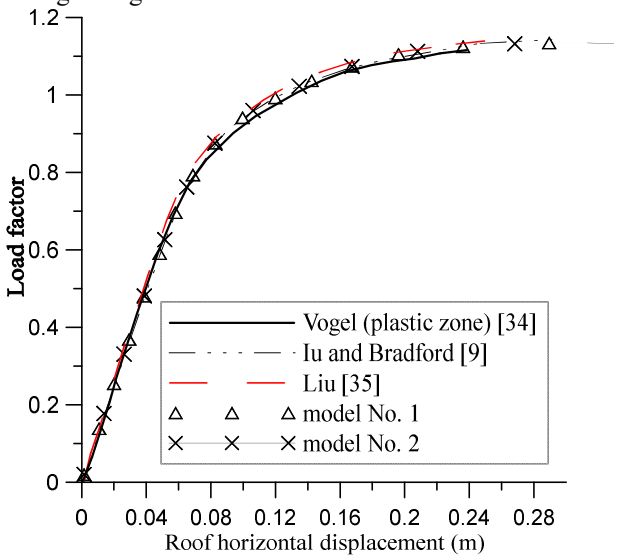

Figure 8: Analysis Results of Vogel's Frame Including Residual Stresses

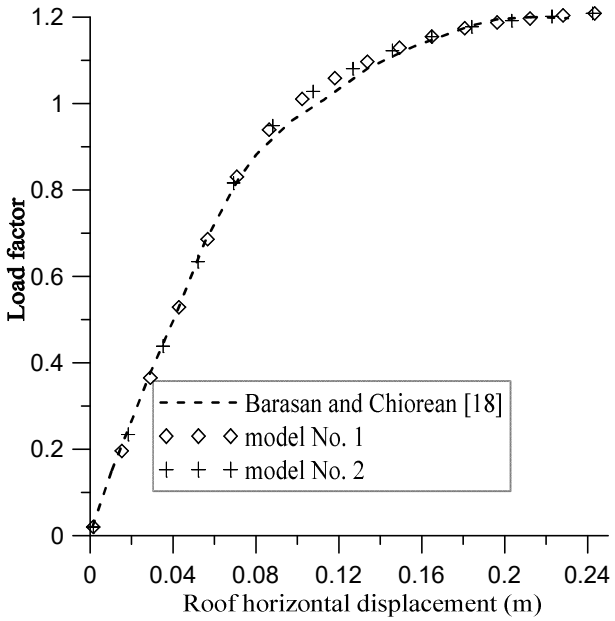

Figure 9: Analysis Results of Vogel's Frame Neglecting Residual Stresses

5.3 Two Story Space Frame with Rectangular Section

The three-dimensional frame in Figure 10 has been solved in many research studies as a part of the evaluation process. This frame has been analyzed by Desoza [24] using force-based methodology to capture geometric and material nonlinearities. Also, the work in [23] employed the same frame to check their proposed model abilities. This frame is solved using our own proposed models and the results are compared to others to assure the accuracy. It's worth mentioning that the members with mid-span concentrated loads is modeled by to elements as nodal forces only are allowed in the current work. The monitored sections are allocated at positions 0.05L, 0.2L, and 0.5L of each end, which guarantees tracing the plasticity at the members. The compared results are presented in Figure 11.

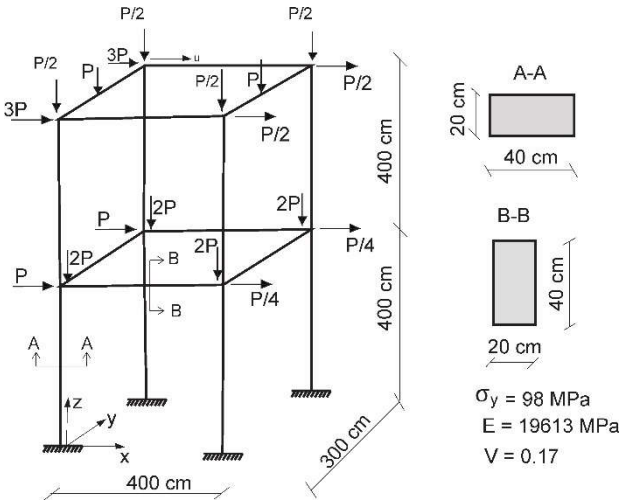

Figure 10: Two Story Space Frame with Rectangular Section

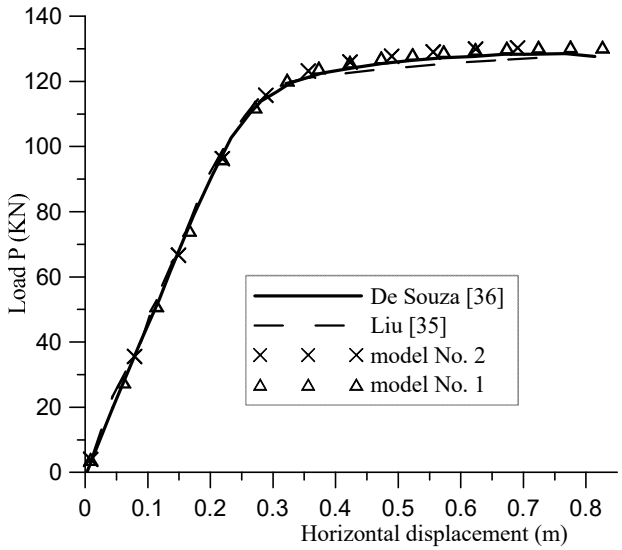

Figure 11: Analysis Results of Two-Story Space Frame with Rectangular Section

5.4 Two Story Space Frame with H-Shaped Section

The steel frame in Figure 12 is an well-known benchmark frame found by Coung and Kim [25]. They presented an accurate solution for the frame with H-shaped cross section using ABAQUS software. Their reference results were based on performing a fine mesh of shell elements with total number of elements equals 49840. The analysis included residual stresses and also geometric imperfections as columns out of plumpness. The value of the force P equals 80 KN. The dimensions of the cross sections is H 150x160x10x6.5, while the material has 320 MPa and 221 GPa for yield stress and elastic modulus, respectively.

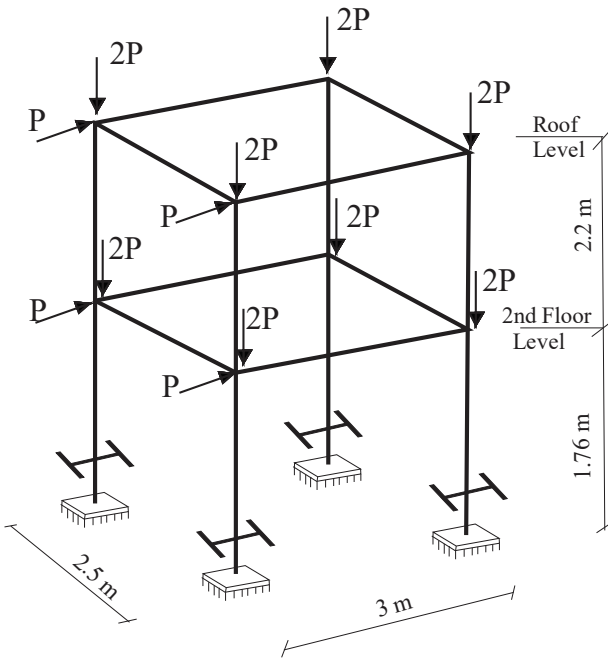

Figure 12: Two Story Space Frame with H-Shaped Section

Detailed information about the geometry of the frame and the modelling of reference solution preparing can be found in [25]. Also, Li *et al.*[26] and Liu [23] performed inelastic analysis for this frame, which also is performed in the present work using a single element per member, considering only 16 frame elements. The monitored sections are poisoned at 0.05L, 0.2L, 0.5L from each node.

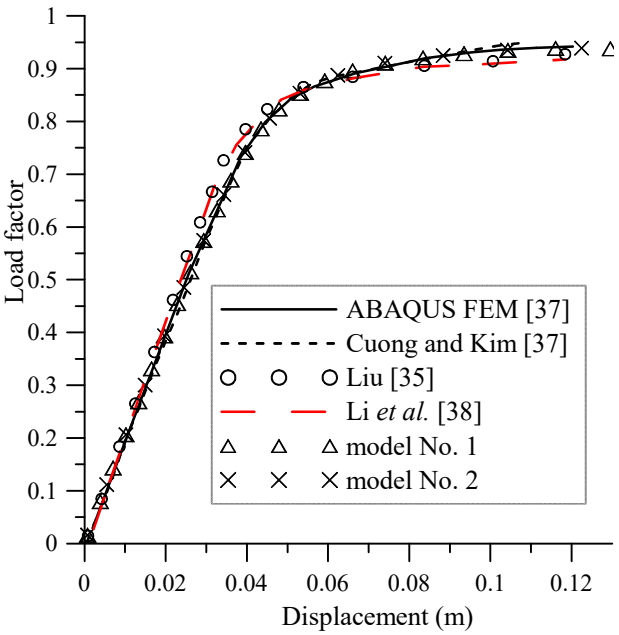

Figure 13: Analysis Results of Two-Story Space Frame with H-Shaped Section

The results for displacements at the roof are presented in Figure 13. Although the work in [23] used three plastic hinges at the member, it seems that the effect of plasticity spread was not captured as accurate as the models of the present work. Which declares the superiority of the present model in tracing geometric and material nonlinear effects.

5.5 Six Story Space Frame

The space frame in Figure 14 has been tried in many researches. The reference solution was provided in [27] using finite element modelling via software USFOS to check their work of improved refined plastic hinge. Also, it has been analyzed by Liu [23] using three hinges model. The results of analysis are compared with the proposed models results. The previously mentioned analysis in [35, 39] required additional span hinges to represent plasticity spread, unlike the proposed models based on one element for member. The curves for the analysis are provided in Figure 15.

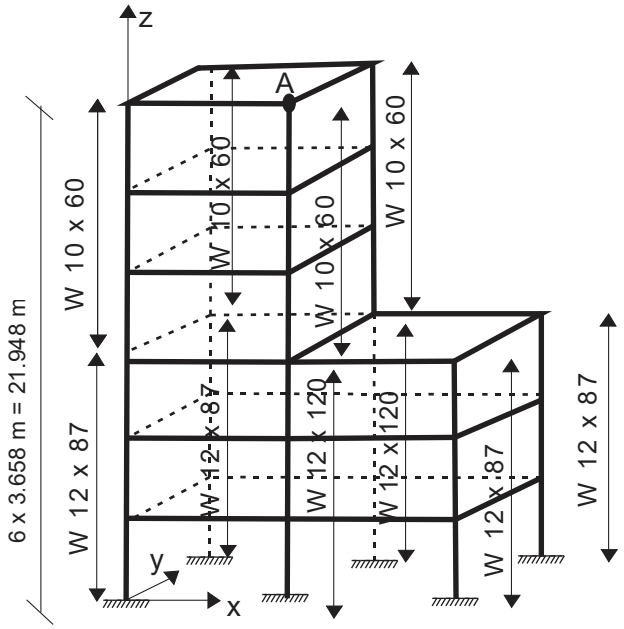

(a)

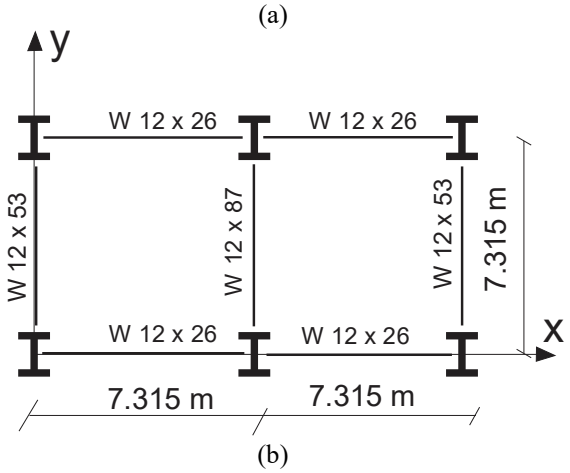

(b)

Figure 14: Geometry of Six Story Space Frame; a) 3-D View, b) Plan

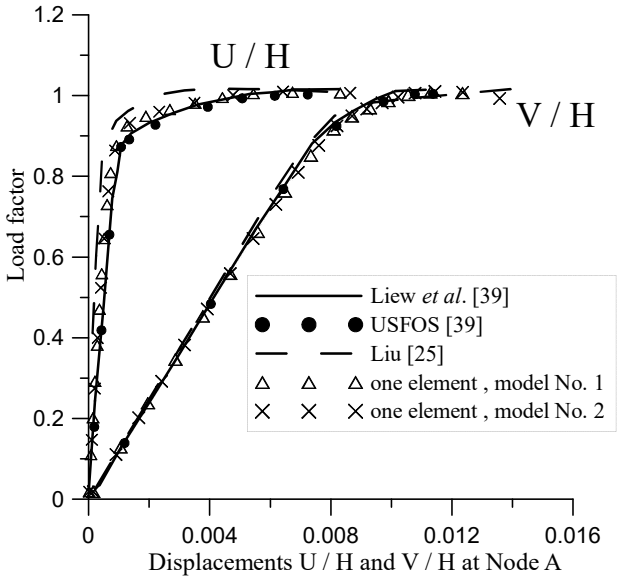

Figure 15: Analysis Results of Six-Story Space Frame

5.6 Cantilever Columns Under Different Circumstances

To assure the reliability of the proposed technique, two cantilever columns of H and I shaped cross sections, in Figure 16, were analyzed. They have been solved with under different loading conditions with different values of member slenderness.

The analysis results are compared with the results when dividing the frame into ten beam-column elements following the plastic zone procedure referred in [8]. Analysis results of a cantilever with I-shaped section with section W250x24 are presented in Figures 17-19. While for a cantilever with H-shaped section with section W250x80, the results are presented in Figures 20-22. The material is assumed to be steel with 500 MPa and 200 GPa for yield stress and elastic modulus, respectively. The figures show the results of one element per member for the present models (1, 2) based on fifth order function and also when using cubic element geometric matrix.

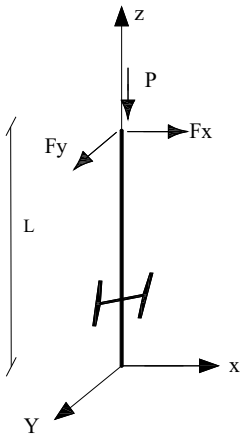

Figure 16: Cantilever Column Under Different Loading Conditions

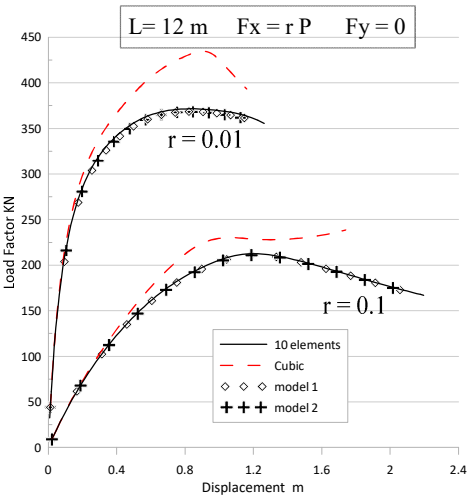

Figure 17: Analysis Results of Cantilever with H-Shaped Section Loaded in Major Axis

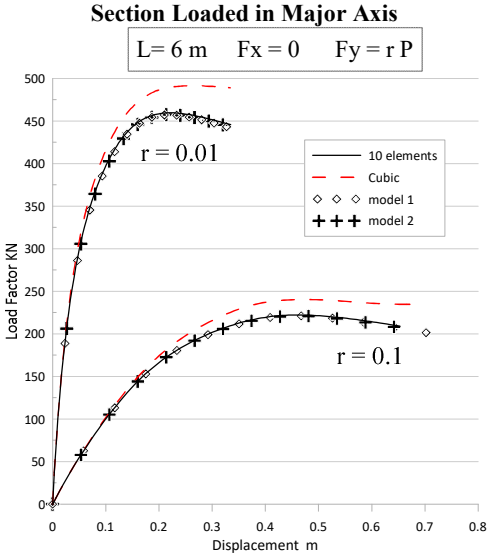

Figure 18: Analysis Results of Cantilever with H-Shaped Section Loaded in Minor Axis

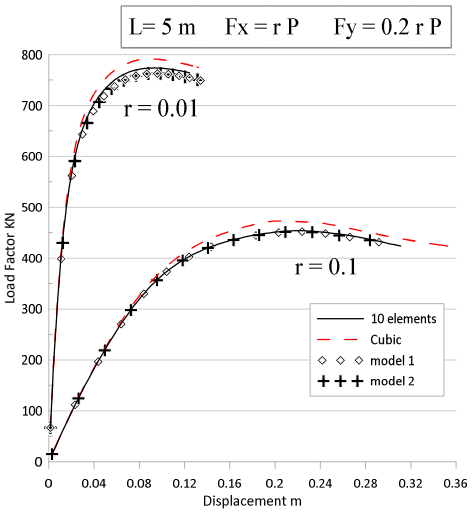

Figure 19: Analysis Results of Cantilever with H-Shaped Section Loaded in Both Axes

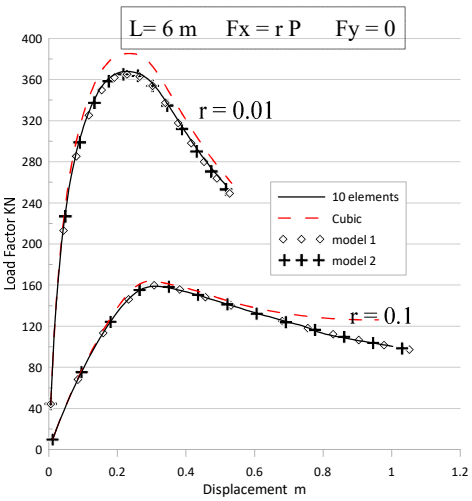

Figure 20: Analysis Results of Cantilever with I-Shaped Section Loaded in Major Axis

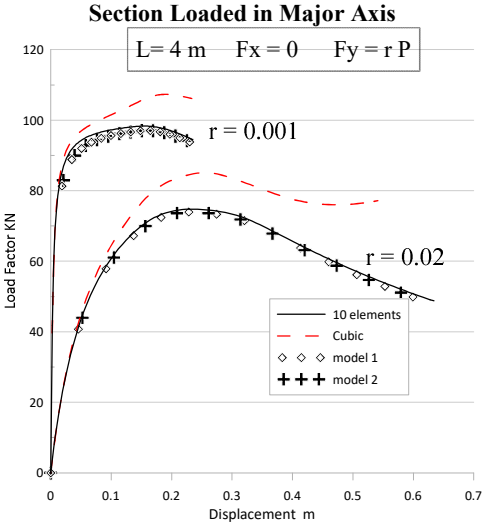

Figure 21: Analysis Results of Cantilever with I-Shaped Section Loaded in Minor Axis

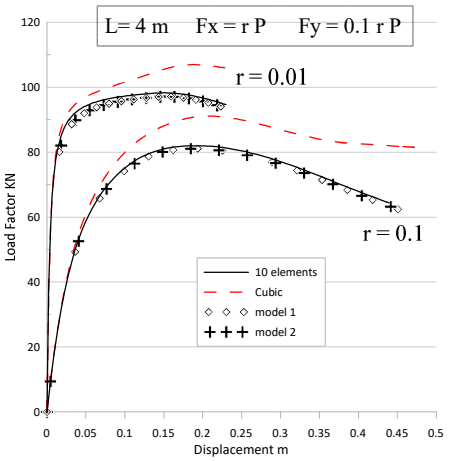

Figure 22: Analysis Results of Cantilever with I-Shaped Section Loaded in Both Axes

6.CONCLUSION

This work presented a beam-column element for second order inelastic analysis of frames. The work employed a displacement function from the fifth order that traced geometric nonlinear behavior accurately. The proposed element included plasticity spread along the member span without dividing the it. The technique used in the analysis employed direct substitution into equations without performing integrations during the analysis neither across the sectional area nor along the element length. The presented element overcame the limitations of lower degrees elements in geometric nonlinearity, and the approximations of plastic hinge analysis. Many solved examples with various plasticity spread cases have been solved to check the model's performance. The results demonstrated that, the model effectively captures both material and geometric nonlinearities while minimizing computational time and storage requirements without compromising accuracy.

7. APPENDIX

$$[\mathrm{T}] = \begin{pmatrix} 0 & \frac{1}{L} & 0 & 0 & 0 & 1 & 0 & -\frac{1}{\mathrm{L}} & 0 & 0 & 0 & 0 \\ 0 & \frac{1}{\mathrm{L}} & 0 & 0 & 0 & 0 & 0 & -\frac{1}{\mathrm{L}} & 0 & 0 & 0 & 1 \\ 0 & 0 & -\frac{1}{\mathrm{L}} & 0 & 1 & 0 & 0 & 0 & \frac{1}{\mathrm{L}} & 0 & 0 & 0 \\ 0 & 0 & -\frac{1}{\mathrm{L}} & 0 & 0 & 0 & 0 & 0 & \frac{1}{\mathrm{L}} & 0 & 1 & 0 \\ 0 & 0 & 0 & -1 & 0 & 0 & 0 & 0 & 0 & 1 & 0 & 0 \\ -1 & 0 & 0 & 0 & 0 & 0 & 1 & 0 & 0 & 0 & 0 & 0 \end{pmatrix} \quad (A.1)$$

T is the matrix transforms [6x6] stiffness matrix to [12x12] including shear stiffness in corotational coordinating approach.

8.REFERENCES

[1] "Specification for Structural Steel Buildings Supersedes the Specification for Structural Steel Buildings," 2022.

[2] T. Cosgun and B. Sayin, "Geometric and material nonlinear analysis of three-dimensional steel frames," International Journal of Steel Structures, vol. 14, no. 1, pp. 59–71, 2014.

[3] T. N. Doan-Ngoc, X. L. Dang, Q. T. Chu, R. J. Balling, and C. Ngo-Huu, "Second-order plastic-hinge analysis of planar steel frames using corotational beam-column element," J Constr Steel Res, vol. 121, pp. 413–426, Jun. 2016.

[4] Jiang, Xiao-Mo, Hong Chen, and JY Richard Liew. "Spread-of-plasticity analysis of three-dimensional steel frames." Journal of Constructional Steel Research 58, no. 2 (2002): 193-212.

[5] S. Lee, T. Kim, Q. X. Lieu, T. P. Vo, and J. Lee, "A novel data-driven analysis for sequentially formulated plastic hinges of steel frames," Comput Struct, vol. 281, Jun. 2023.

[6] Ziemian, Ronald D., and William McGuire. "Modified tangent modulus approach, a contribution to plastic hinge analysis." Journal of Structural Engineering 128.10 (2002): 1301-1307.
[7] Alvarenga, Arthur R., and Ricardo AM Silveira. "Second-order plastic-zone analysis of steel frames Part I: Numerical formulation and examples of validation." Latin American Journal of Solids and Structures 6.2 (2009): 132-152.
[8] B. Le-Van, C. G. Chiorean, S. E. Kim, and C. Ngo-Huu, "Nonlinear inelastic analysis of space semi-rigid steel frames subjected to static load using plastic-zone method," Mechanics of Advanced Materials and Structures, Oct. 2023.
[9] Iu, Chin Kin, and M. Bradford. "Higher-order non-linear analysis of steel structures. Part II: refined plastic hinge formulation." Advanced Steel Construction 8, no. 2 (2012): 183-198.
[10] H. K. Dang, D. K. Thai, and S. E. Kim, "Stochastic analysis of semi-rigid steel frames using a refined plastic-hinge model and Latin hypercube sampling," Eng Struct, vol. 291, Sep. 2023.
[11] Liew, J. Y. R., and W. F. Chen. "Implications of using refined plastic hinge analysis for load and resistance factor design." Thin-walled structures 20.1-4 (1994): 17-47.
[12] Y. Zhou, D. Huang, T. Li, and Y. Li, "Second-order arbitrarily-located-refined plastic hinge model for high-strength steel frame design," J Constr Steel Res, vol. 190, Mar. 2022.
[13] Y. Zhou, B. Hu, Y. Gong, L. Tang, and Y. Li, "Second-order improved refined plastic hinge method with implementation of continuous strength method," J Constr Steel Res, vol. 211, Dec. 2023.
[14] Thai, Huu-Tai, et al. "Review of nonlinear analysis and modeling of steel and composite structures." International Journal of Structural Stability and Dynamics 20.04 (2020): 2030003.
[15] H. F. Viana, R. G. L. da Silva, R. S. Costa, and A. C. C. Lavall, "Formulation for nonlinear dynamic analysis of steel frames considering the plastic zone method," Eng Struct, vol. 223, Nov. 2020.
[16] H. T. Thai and S. E. Kim, "Second-order distributed plasticity analysis of steel frames with semi-rigid connections," Thin-Walled Structures, vol. 94, pp. 120–128, Sep. 2015.
[17] S. Shayan, K. J. R. Rasmussen, and H. Zhang, "Probabilistic modelling of residual stress in advanced analysis of steel structures," J Constr Steel Res, vol. 101, pp. 407–414, 2014.
[18] G. M. Barsan and C. G. Chiorean, "Influence of residual stress on the carrying-capacity of steel framed structures. Numerical investigation," In: Dubina D, Ivany M, editors. Stability and ductility of steel structures. Elsevier, pp. 317–324, 1999.
[19] Z. L. Du, Y. P. Liu, and S. L. Chan, "A force-based element for direct analysis using stress-resultant plasticity model," Steel and Composite Structures, vol. 29, no. 2, pp. 175–186, Oct. 2018.
[20] Z. L. Du, Z. X. Ding, Y. P. Liu, and S. L. Chan, "Advanced flexibility-based beam-column element allowing for shear deformation and initial imperfection for direct analysis," Eng Struct, vol. 199, Nov. 2019.
[21] A. H. Zubydan, "Inelastic large deflection analysis of space steel frames including H-shaped cross-sectional members," Eng Struct, vol. 48, pp. 155–165, Mar. 2013.
[22] A. ElSabbagh, A. Hanefa, A. Zubydan, M. ElGhandour, and T. Sharaf, "Inelastic large deflection analysis of space steel frames consisting of I-shaped cross section," Steel and Composite Structures, vol. 41, no. 6, pp. 887–898, Dec. 2021.
[23] C. Oran, "Tangent Stiffness in Space Frames," Journal of the Structural Division, vol. 99, no. 6, pp. 987–1001, Jun. 1973.
[24] H. T. Thai and S. E. Kim, "Practical advanced analysis software for nonlinear inelastic analysis of space steel structures," Advances in Engineering Software, vol. 40, no. 9, pp. 786–797, 2009.
[25] Teh, Lip H. "Cubic beam elements in practical analysis and design of steel frames." Engineering structures 23.10 (2001): 1243-1255.
[26] Chan, Siu Lai, and Zhi Hua Zhou. "Pointwise equilibrating polynomial element for nonlinear analysis of frames." Journal of structural engineering 120.6 (1994): 1703-1717.
[27] C. K. Iu and M. A. Bradford, "Second-order elastic finite element analysis of steel structures using a single element per member," Eng Struct, vol. 32, no. 9, pp. 2606–2616, Sep. 2010.
[28] A. H. Zubydan, A. I. ElSabbagh, T. Sharaf, and A. E. Farag, "Inelastic large deflection analysis of space steel frames using an equivalent accumulated element," Eng Struct, vol. 162, pp. 121–134, May 2018.
[29] Y. Q. Tang, H. Zhu, Y. P. Liu, Y. Y. Ding, and S. L. Chan, "A novel efficient plastic hinge approach for direct analysis of steel structures," Eng Struct, vol. 319, Nov. 2024.
[30] A. H. Zubydan, "A simplified model for inelastic second order analysis of planar frames," Eng Struct, vol. 32, no. 10, pp. 3258–3268, Oct. 2010.
[31] A. H. Zubydan, "Inelastic second order analysis of steel frame elements flexed about minor axis," Eng Struct, vol. 33, no. 4, pp. 1240–1250, Apr. 2011.
[32] T. Sharaf, A. Hanefa, A. Zubydan, M. Elghandour, and A. Elsabbagh, "Axial Force and Biaxial Bending Interaction for I-Shaped Cross Section," Practice Periodical on Structural Design and Construction, vol. 26, no. 4, Nov. 2021.
[33] H. T. Thai and S. E. Kim, "Nonlinear inelastic analysis of space frames," J Constr Steel Res, vol. 67, no. 4, pp. 585–592, Apr. 2011.

[34] Vogel, U., 1985. Calibrating frames. Stahlbau, 10(10), pp.1-7.
[35] Liu, Siwei. "Second-order design and advanced analysis of hybrid steel and concrete framed structures." PhD, The Hong Kong Polytechnic University, Hong Kong, 2013.
[36] R. Magalhães De Souza, "Force-based Finite Element for Large Displacement Inelastic Analysis of Frames,",PhD, The University of California, Berkeley, 2000.
[37] C. Ngo-Huu and S. E. Kim, "Practical advanced analysis of space steel frames using fiber hinge method," Thin-Walled Structures, vol. 47, no. 4, pp. 421–430, Apr. 2009.
[38] T. J. Li, S. W. Liu, and S. L. Chan, "Direct analysis for high-strength steel frames with explicit-model of residual stresses," Eng Struct, vol. 100, pp. 342–355, Oct. 2015.
[39] Liew, JY Richard, et al. "Improved nonlinear plastic hinge analysis of space frame structures." Engineering structures 22.10 (2000): 1324-1338.